Akimotoite, (Mg,Fe)SiO₃, a new silicate mineral of the ilmenite group in the Tenham chondrite

Naotaka Tomioka* and Kiyoshi Fujino

Division of Earth and Planetary Sciences, Graduate School of Science, Hokaido University, Sapporo 060–0810, Japan

Abstract

Akimotoite, (Mg,Fe)SiO₃, a new silicate mineral of the ilmenite group, was found in the shock-metamorphosed Tenham chondrite. It occurs as aggregates adjacent to clinoenstatite in fragments within shock-induced melt veins. Chemical analyses show the simplified formula to be $(Mg_{0.79}Fe_{0.21})SiO_3$, the same as for clinoenstatite. Selected-area electron diffraction (SAED) patterns correspond to the synthetic (Mg,Fe)SiO₃ ilmenite phase with space group $R\bar{3}$. Lattice parameters derived from SAED patterns are a = 0.478(5) nm, c = 1.36(1) nm and V = 0.269(8) nm³ in the hexagonal setting. The calculated density is 4.0(1) g/cm³. Akimotoite in this occurrence is thought to have been transformed from original orthoenstatite in a solid-state reaction produced by a shock event. Peak pressure and temperature generated by shock events in Tenham are estimated to be 22 GPa $<P_{max}$ < 26 GPa and T_{max} >2000 °C, assuming that equilibrium crystallization of aluminous majorite occurred in the melt veins. This new mineral was named after Syun-iti Akimoto.

Introduction

The ilmenite structure is one of the high-pressure polymorphs of enstatite first synthesized by Kawai et al. (1974): Liu (1976) determined that it has the ilmenite structure. Subsequently, the stability field of the ilmenite-structure polymorph was investigated by ultra-high-pressure experiments in the systems MgSiO₃ (Ito and Navrotsky 1985; Sawamoto 1987; Ito and Takahashi 1989; Yusa et al. 1993), MgSiO₃-FeSiO₃ (Ito and Yamada 1982), and MgSiO₃-Al₂O₃ (Kanzaki 1987; Irifune and Ringwood 1987; Gasparik 1990). The MgSiO₃ ilmenite phase is stable only at very high pressures of ≥20 GPa (Sawamoto 1987). Therefore, the ilmenite phase could be the major constituent minerals of the transition zone and the lower mantle of the Earth.

Although several high-pressure silicate phases have been found in shocked meteorites, natural occurrence of the high pressure polymorphs of pyroxene had been limited only to the garnet phase majorite (Smith and Mason 1970). Recently, Sharp et al. (1997) and Tomioka and Fujino (1997) independently discovered the natural silicate ilmenite phase in shocked meteorites. Additionally, a natural silicate perovskite phase in the Tenham meteorite was found. These high-pressure silicate minerals in meteorites are very important for understanding not only the shock metamorphism of meteorites, but also the nature of the constituent minerals of the deep mantle. This paper describes the natural occurrence, chemical composition, crystallography, and possible formation mechanism of the (Mg,Fe)SiO₃ ilmenite phase found in the Tenham chondrite, as compared to that in the Acfer 040 chondrite reported by Sharp et al. (1997).

This ilmenite phase was approved by the Commission on New Minerals and Mineral Names, International Mineralogical Association as a new mineral with the mineral name akimotoite. The mineral name is after Syun-iti Akimoto in honor of his great contributions to high-pressure research.

Occurrence

The Tenham chondritic meteorite (L6) fell in 1879 in South Gregory, Queensland, Australia (25°44′S, 142°57′E) (Spencer 1937). This meteorite consists mainly of olivine, orthoenstatite, diopside, plagioclase that has been partly converted to diaplectic glass (maskelynite), Fe-Ni alloy, and troilite. It was very strongly shocked (shock stage of S6 by Stöffler et al. 1991), and a network of shock-induced melt veins ≤1 mm in width runs across the entire body (Fig. 1). Host minerals are enclosed as multiphase fragments in shock veins and are partially or totally transformed into high-pressure phases. Olivine in the walls of the veins is also partially converted to blue ringwoodite. The black matrix of the vein is dominated by aluminous majorite and lesser magnesiowüstite, Fe-metal, Fe-oxide, and Fe-sulfide. Detailed descriptions of the Tenham chondrite and its shock veins were previously reported by Price et al. (1979) and Langenhorst et al. (1995).

Akimotoite cannot be identified through an optical microscope due to its very small size and low abundance. Therefore, observations were mainly carried out using an analytical transmission electron microscope (ATEM). ATEM specimens were prepared as follows: Molybde-
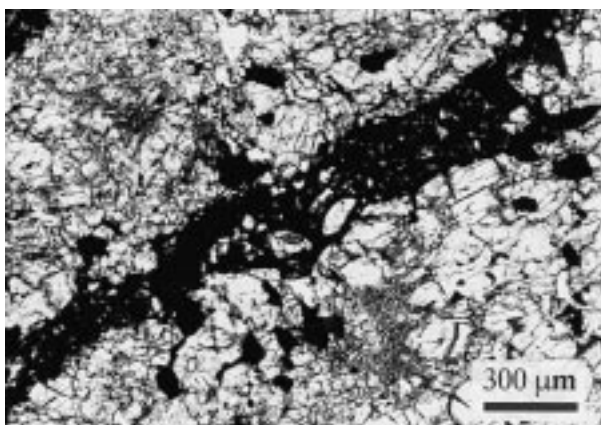
FIGURE 1. Photomicrograph of shock-induced veins in the Tenham chondrite. Many fragments are enclosed within the shock vein. The black matrix consists of very fine-grained crystalline majorite, magnesiowüstite, Fe-metal, Fe-oxide, and Fe-sulfide grains.

num rings were glued with epoxy on selected parts of a 30 µm thin section that was glued to a glass slide with Lakeside cement. The rings and the enclosed areas were then cut from the section, heated to 120 °C, and promptly removed from the slide glass. Subsequently, these specimens were milled into ATEM thin foils by Ar-ion milling at 4 kV and 0.8 mA and coated with carbon.

Electron microscope examination of three shock veins revealed that in one vein akimotoite existed as aggregates adjacent to clinoenstatite (converted from orthoenstatite by the shock event) in fragments. Akimotoite grains in the procured Tenham chondrite sample have two morphologies; one is granular (<0.4 µm) and the other columnar (<1.4 µm in length) (Fig. 2). Neither grain type showed any particular microstructure except for a low density of dislocations. Granular grains were sometimes separated by glassy rims several tens of nanometers in width, which have almost the same composition as akimotoite. These amorphous rims in akimotoite grains were perhaps formed by a solid-state reaction during shock compression, or partial amorphization of akimotoite by electron-beam irradiation or ion thinning. The assemblage of columnar grains has a brick-wall-like texture, and most columnar grains have a topotaxial relationship with adjacent clinoenstatite: $(0001)_{Ak}$ and $(10\bar{1}0)_{Ak}$ are almost parallel to $(100)_{Cen}$ and $(010)_{Cen}$ (Ak = akimotoite and Cen = clinoenstatite), respectively. In the second vein, akimotoite intergrown with clinoenstatite was observed (Fig. 3). This intergrowth also exhibited the same topotaxial relationship. No akimotoite was found in the third vein.

Silicate perovskite grains were also found in the same mode of occurrence as granular akimotoite. This perovskite phase was also adjacent to clinoenstatite in a fragment in the melt vein, and its selected area electron diffraction (SAED) pattern indicated an orthorhombic perovskite structure (Tomioka and Fujino 1997). Silicate perovskite has not yet been given a mineral name.
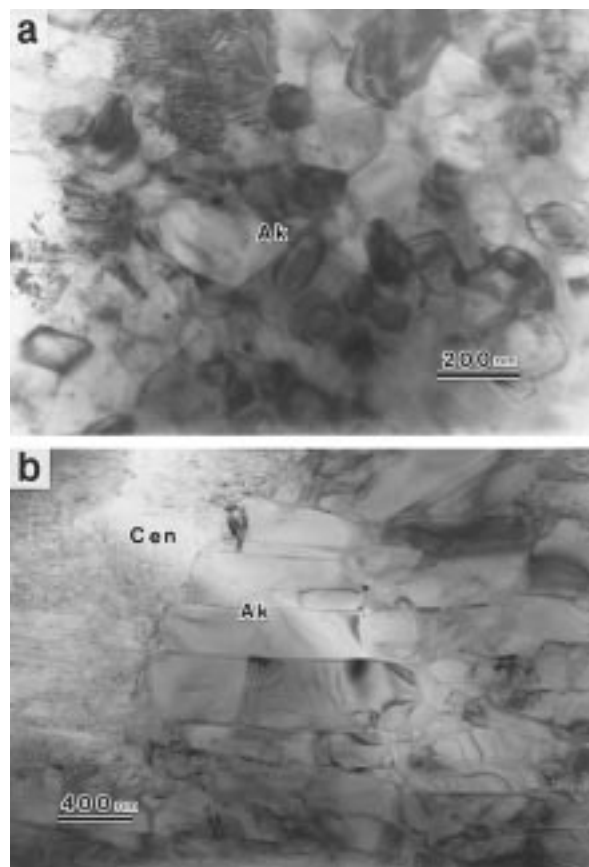

FIGURE 2. Electron micrograph of akimotoite (Ak). (**a**) Granular grains. (**b**) Columnar grains. Aggregates of akimotoite are adjacent to a large clinoenstatite grain (Cen) with (100) twin lamallae.

CHEMICAL COMPOSITION AND CRYSTALLOGRAPHY

Chemical compositions of akimotoite, silicate perovskite, and majorite in the Tenham chondrite were obtained with an energy-dispersive X-ray spectrometer attached to the TEM; compositions of clinoenstatite were obtained with an electron probe microanalyzer. Compositions for akimotoite, silicate perovskite, and majorite were calculated by using experimentally determined Cliff-Lorimer factors k. The analytical procedure for ATEM is reported in Fujino et al. (1998). The compositions of akimotoite, silicate perovskite, majorite, and clinoenstatite obtained here are listed in Table 1 together with those of akimotoite and amorphized silicate perovskite reported by Sharp et al. (1997).

Both akimotoite and silicate perovskite in the present study have almost the same chemical composition as clinoenstatite, and their formulae can be approximated by $(Mg_{0.78-0.79},Fe_{0.22-0.21})SiO_3$. The $FeSiO_3$ content of more than 20 mol% in akimotoite is significantly higher than that for synthetic samples reported previously (Ito and Yamada 1982).

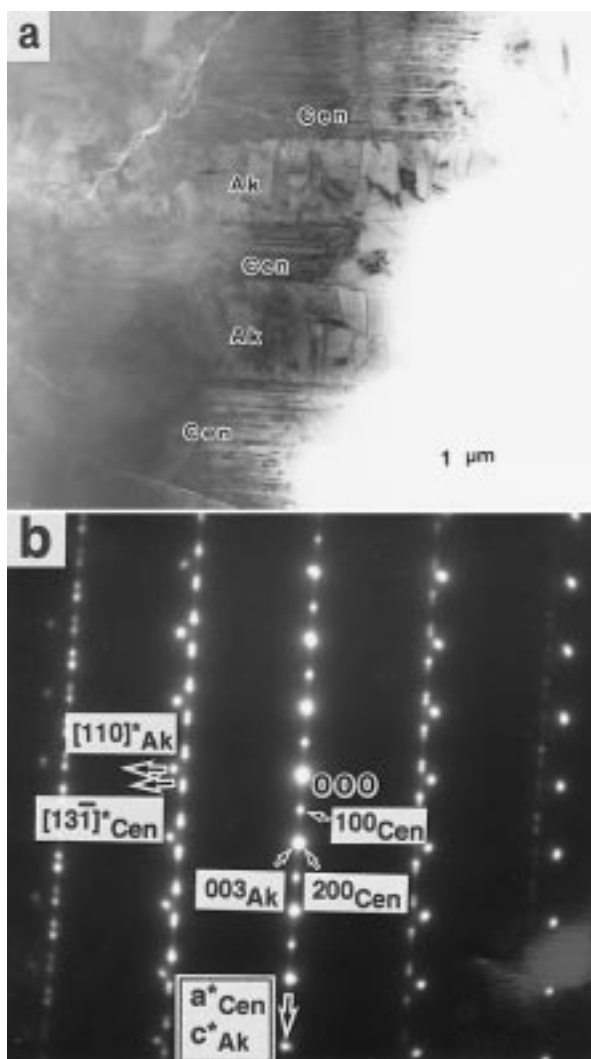Crystallographic data for akimotoite were obtained

FIGURE 3. Intergrowth of akimotoite with clinoenstatite. (**a**) Electron micrograph. Transverse fractures are common in the akimotoite. (**b**) SAED pattern taken from the area including both clinenstatite and akimotoite in **a**. This pattern shows a topotaxial relationship: $(0001)_{Ak}$ is just parallel to $(100)_{Cen}$ in this case.

TABLE 1. Chemical compositions of akimotoite and other polymorphs of pyroxene in shocked chondrites by analytical electron microscopy

(wt%)	Tenham				Acfer 040*	
	Cen†	Ak	Pv	Maj	Ak	Pv‡
Na_2O	0.01	0.67	0.81	0.76	0.42	2.02
MgO	29.33	28.39	28.58	25.59	35.34	26.24
Al_2O_3	0.15	0.07	0.16	4.57	4.44	4.69
SiO_2	55.74	56.35	55.14	56.08	55.54	49.14
CaO	0.78	0.38	0.12	2.12		3.95
TiO_2	0.15	0.17	0.42	0.11		
Cr_2O_3	0.16	0.16	0.18	0.47	0.50	tr
MnO	0.51	0.28	0.19	0.27		0.81
FeO	13.51	13.54	14.41	10.03	3.72	13.16
Total	100.33	100	100	100	100	100
(Cation number O = 12)						
Na	0.00	0.09	0.11	0.10	0.06	0.29
Mg	3.11	3.02	3.06	2.68	3.60	2.87
Al	0.01	0.01	0.01	0.38	0.36	0.36
Si	3.97	4.02	3.96	3.94	3.79	3.61
Ca	0.06	0.03	0.01	0.16		0.31
Ti	0.01	0.01	0.02	0.01		
Cr	0.01	0.01	0.01	0.03	0.03	
Mn	0.03	0.02	0.01	0.02		0.05
Fe	0.81	0.81	0.87	0.59	0.21	0.81
Fe/(Mg+Fe)	0.21	0.21	0.22	0.18	0.06	0.22

Notes: Abbreviations: Cen = clinoenstatite, Ak = akimotoite, Pv = silicate perovskite, Maj = majorite, tr = trace. Oxide contents (upper section) in wt%. Cation numbers (lower section) assume 12 O atoms.
* Data from Sharp et al. (1997).
† Determined by electron microprobe analysis.
‡ Amorphous material inferred to have been silicate perovskite.

physical properties could not be obtained due to the small amounts present and the very fine grain size.

DISCUSSION

The mode of occurrence of akimotoite and silicate perovskite in the Tenham chondrite is different from that in the Acfer 040 chondrite in several respects: (1) In Tenham, akimotoite and silicate perovskite were found inside enstatite fragments in the shock veins, whereas Sharp et al. (1997) reported akimotoite, amorphous grains (assumed to be amorphized silicate perovskite) and ringwoodite constituting the matrix of shock veins of Acfer 040. (2) Akimotoite and silicate perovskite in Tenham have similar chemical compositions as that of adjacent clinoenstatite, almost (Mg,Fe)SiO₃, while akimotoite and amorphized silicate perovskite in Acfer 040 contain significant amounts of Al_2O_3 in common, plus Cr_2O_3 (akimotoite) or CaO and Na_2O (silicate perovskite) (Table 1). (3) Akimotoite and silicate perovskite in Tenham are very fine-grained (less than ~0.4 μm for granular grains), whereas those in Acfer 040 are up to ~2 μm in size. (4) In Tenham, no interstitial phase exists among akimotoite or perovskite grains, whereas the interstices of predominant amorphized perovskite in Acfer 040 were filled with finer-grained akimotoite, ringwoodite, and glass.

The above observations suggest two mechanisms for the formation of akimotoite and silicate perovskite in the shocked chondrites. In the case of the Tenham chondrite, akimotoite and silicate perovskite seem to have been transformed by a solid-state transformation directly from
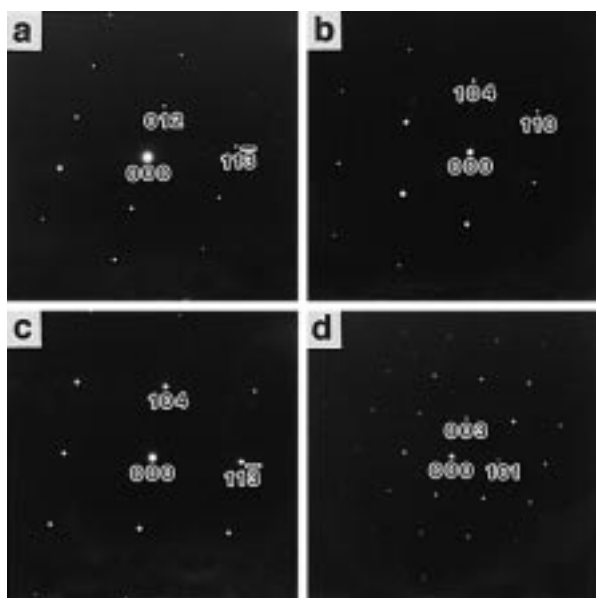
from nine electron micrographs of the SAED patterns (Fig. 4). The SAED patterns showed that akimotoite has trigonal symmetry with space group $R\bar{3}$. Lattice parameters were a = 0.478(5) nm, c = 1.36(1) nm, V = 0.269(8) nm³ in the hexagonal setting, and the calculated density was 4.0(1) g/cm³. Because of multiple diffraction, distinguishing space group $R\bar{3}$ for the ilmenite structure from $R\bar{3}c$ for the corundum structure was somewhat difficult. In the present case, however, the 003 reflection remained when the specimen was tilted from the zone-axis orientation. This suggests that the 003 spot is not due to multiple diffraction, and that akimotoite belongs to $R\bar{3}$ (diffraction conditions; l = 3n for 00l in $R\bar{3}$ and l = 6n for 00l in $R\bar{3}c$ where n is an integer). Optical and

FIGURE 4. Selected electron micrographs of SAED patterns of akimotoite. SAED patterns of **a** and **b** were taken from the same grain.

host enstatite, whereas Sharp et al. (1997) suggested that akimotoite and silicate perovskite in Acfer 040 crystallized from shock-induced melt. However, aluminous majorite grains observed as the predominant phase in the matrix of shock veins in Tenham strongly resemble the amorphized silicate perovskite grains in Acfer 040 in respect to the facts listed above, and are, therefore, thought to have crystallized from melt.

Sharp et al. (1997) estimated, based on the stability of $MgSiO_3$-perovskite in the Allende chondrite (Agee et al. 1995), that crystallization of melt veins in Acfer 040 began at a pressure and temperature in excess of 26 GPa and 2000 °C by assuming that silicate perovskite was the liquidus phase. In contrast, the dominant phase in the matrix of the shock veins in Tenham is aluminous majorite, and according to the phase diagram for the Allende chondrite (Agee et al. 1995), majorite is the liquidus phase in the range of 14 to 26 GPa. Therefore, if the phase diagram for Allende can be applied to the Tenham chondrite, crystallization of melt veins in Tenham probably occurred at pressures of 14 to 26 GPa. Existence of $(Mg,Fe)SiO_3$ perovskite in a fragment that transformed in a solid state means that the lower limit of maximum pressure generated by the shock event will be higher than the lower limit of the stability field of perovskite. In the phase diagram of $MgSiO_3$ by Yusa et al. (1993), the stability field of silicate perovskite is ≥ 22 GPa. The lower limit for pressure of that field increases with the Fe content (Ito and Yamada 1982). Therefore, peak pressure of the shock veins generated by the shock events in Tenham is estimated to be in the range of 22 to 26 GPa, assuming equilibrium crystallization of aluminous majorite. The corresponding peak temperature will be higher than 2000 °C.

Chemical analyses show that akimotoite and silicate perovskite in this study have 21 to 22 mol% $FeSiO_3$. However, according to the phase equilibrium studies, the solubility limits of $FeSiO_3$ in Al-free akimotoite and silicate perovskite are much lower at pressures 22 to 26 GPa. Ito and Yamada (1982) report that the solubility limit for akimotoite is less than ~13 mol% at pressure 22 to 26 GPa and at 1100 °C, and Mao et al. (1997) report that the limit for silicate perovskite is less than 14 mol% at pressures <26 GPa and temperatures <1727 °C. Considering the higher Fe contents observed here, these two reports suggest that at equilibrium under pressures 22 to 26 GPa, single-phase akimotoite and silicate perovskite would be replaced by γ-spinel + stishovite and silicate perovskite + magnesiowüstite + stishovite. Nevertheless, such decomposition was not observed around the akimotoite or silicate perovskite grains. In a short shock event, therefore, solid-state decomposition may be kinetically hindered, and enstatite may transform metastably into akimotoite or silicate perovskite containing excess Fe, without producing the stable phases. Alternatively, achievement of higher temperatures in the meteorite than in the syntheses could promote higher solubility of Fe.

Intergrowth of akimotoite with clinoenstatite was observed in one of the three veins examined, and both phases have a topotaxial relationship; the (0001) plane of akimotoite is just parallel to the (100) plane of clinoenstatite in some cases, or nearly parallel in others (Fig. 3b). These planes correspond to the layers of the nearly close-packed O atoms for both structures. This feature seems to suggest that the transition from enstatite to columnar akimotoite was caused by a martensitic-type shear transformation mechanism. However, the topotaxy between both phases was not always strict (Tomioka and Fujino 1997), and frequent stacking faults parallel to (0001) were so far not observed in akimotoite. Moreover, Kerschhofer et al. (1996) reported an example of intracrystalline nucleation and growth of γ-spinel on shear-induced stacking faults in olivine where both phases have a topotaxial relationship. Therefore, at the present stage, the exact mechanism of the enstatite-akimotoite transition with a topotaxial relationship is not clear. Further examination of the microstructures at the enstatite-akimotoite interface is required. The controlling factors to produce the difference of columnar and granular morphologies of akimotoite are also not clear at the present stage, although morphology may be related to the degree of differential stress, cooling rate, or overpressure.

References cited

Agee, C.B., Li, J., Shannon, M.C., and Circone, S. (1995) Pressure-temperature phase diagram for the Allende meteorite. Journal of Geophysical Research, 100, 17725–17740.

Fujino, K., Miyajima, N., Yagi, T., Kondo, T., and Funamori, N. (1998) Analytical electron microscopy of the garnet-perovskite transformation in a laser-heated diamond anvil cell. In M.H. Manghnani and T. Yagi, Eds., Properties of Earth and Planetary Materials at High Pressure and Temperature, p. 409–417. American Geophysical Union, Washington DC.

Gasparik, T. (1990) Phase relations in the transition zone. Journal of Geophysical Research, 95, 15751–15769.

Irifune, T. and Ringwood, A.E. (1987) Phase transformations in a harzburgite composition to 26 GPa: implications for dynamical behavior of the subducting slab. Earth and Planetary Science Letters, 86, 365–376.

Ito, E. and Navrotsky, A. (1985) $MgSiO_3$ ilmenite: calorimetry, phase equilibria, and decomposition at atmospheric pressure. American Mineralogist, 70, 1020–1026.

Ito, E. and Takahashi, E. (1989) Postspinel transformations in the system Mg_2SiO_4-Fe_2SiO_4 and some geophysical implications. Journal of Geophysical Research, 94, 10637–10646.

Ito, E. and Yamada, H. (1982) Stability relations of silicate spinels, ilmenites, and perovskites. In S. Akimoto and M.H. Manghnani, Eds., High-Pressure Research in Geophysics, p. 405–419. Center of Academic Publications, Tokyo.

Kanzaki, M. (1987) Ultra-high-pressure phase relations in the system $Mg_4Si_4O_{12}$-$Mg_3Al_2Si_3O_{12}$. Physics of the Earth and Planetary Interiors, 49, 168–175.

Kawai, N., Tachimori, M., and Ito. E. (1974) A high-pressure hexagonal form of $MgSiO_3$. Proceedings of the Japan Academy, 50, 378–380.

Kerschofer, L., Sharp T.G., and Rubie, D.C. (1996) Intracrystalline transformation of olivine to wadsleyite and ringwoodite under subduction zone conditions. Science, 274, 79–81.

Langenhorst, F., Joreau P., and Doukhan, J.C. (1995) Thermal and shock metamorphism of the Tenham chondrite: A TEM examination. Geochimica et Cosmochimica Acta, 59, 1835–1845.

Liu, L.G. (1976) The high-pressure phases of $MgSiO_3$. Earth and Planetary Science Letters, 31, 200–208.

Mao, H.K., Shen, G., and Hemley, R.J. (1997) Multivariable dependence of Fe-Mg partioning in the lower mantle. Science, 278, 2098–2100.

Price, G.D., Putnis, A., and Agrell, S.O. (1979) Electron petrography of shock-produced veins in the Tenham chondrite. Contributions to Mineralogy and Petrology, 71, 211–218.

Sawamoto, H. (1987) Phase diagram of $MgSiO_3$ at pressures up to 24 GPa and temperatures up to 2200 °C: phase stability and properties of tetragonal garnet. In M.H. Manghnani and Y. Syono, Eds., High-Pressure Research in Mineral Physics, 209–219, American Geophysical Union, Washington, D.C.

Sharp, T.G., Lingemann, C.M. Dupas, C., and Stöffler, D. (1997) Natural occurrence of $MgSiO_3$-ilmenite and evidence for $MgSiO_3$-perovskite in a shocked L chondrite. Science, 277, 352–355.

Smith, J.V. and Mason, B. (1970) Pyroxene-garnet transformation in Coorara meteorite. Science, 168, 832–833.

Stöffler, D., Keil, K., and Scott, E.R.D. (1991) Shock metamorphism of ordinary chondrites. Geochimica et Cosmochimica Acta, 55, 3845–3867.

Spencer, L.J. (1937) The Tenham (Queensland) meteoritic shower of 1879. Mineralogical Magazine, 24, 437–452.

Tomioka, N. and Fujino, K. (1997) Natural (Mg, Fe)SiO_3-ilmenite and -perovskite in the Tenham meteorite. Science, 277, 1084–1086.

Yusa, H., Akaogi, M., and Ito, E. (1993) Calorimetric study of $MgSiO_3$ garnet and pyroxene: heat capacities, transition enthalpies, and equilibrium phase relations in $MgSiO_3$ at high pressures and temperatures. Journal of Geophysical Research, 98, 6453–6460.